Quantitative Aggregation of Microbiome Sequencing Data Provides Insights into the Associations between the Skin Microbiome and Psoriasis

Alfred A. Chan[1], Patrick T. Tran[2] and Delphine J. Lee[1,2,3]

Although prior studies have reported distinct skin microbiome profiles associated with psoriasis, differences in methods and analyses limit generalizable conclusions. Individual studies have actually reported conflicting findings; for example, *Propionibacterium* and *Staphylococcus* have been significantly associated with both psoriatic lesions and healthy skin. Qualitative reviews have attempted to summarize this body of work, but there is great variability across the studies' findings and methods. To better unify these data, we created a meta-analysis of all publicly available datasets by utilizing a uniform bioinformatics pipeline and reference database to investigate associations of the skin microbiome in psoriasis. A total of 977 skin swab samples (341 lesional, 295 nonlesional, and 341 healthy) from 6 studies were analyzed. The aggregated analysis revealed a higher relative abundance of microorganisms, including *Staphylococcus aureus* and *Corynebacterium simulans*, among others, from patients with psoriasis than those from healthy swab samples; in addition, *Cutibacterium acnes*, *Lawsonella* unclassified, and *S warneri* were significantly higher in healthy samples. Furthermore, comparison of functional pathways predicted from 16S gene markers showed that L-ornithine biosynthesis and L-histidine biosynthesis were lower in psoriatic lesions than in healthy controls. Taken together, this meta-analysis allows for a more generalizable association between the skin microbiome and psoriasis.

Keywords: 16S, Meta-analysis, Metagenomics, Microbiome, Psoriasis

JID Innovations (2024);**4:**100249 doi:10.1016/j.xjidi.2023.100249

INTRODUCTION

Psoriasis affects the health of many people worldwide. The pathogenesis of psoriasis is multifactorial, and the role of the skin microbiome in psoriasis is still being studied. Prior studies have reported distinct skin microbiome profiles associated with psoriatic lesions (Chen et al, 2020), and qualitative reviews have attempted to summarize these studies (Carmona-Cruz et al, 2022; Lewis et al, 2019; Mazur et al, 2021). However, differences in how the samples were obtained and analyzed limit what can be concluded (Lewis et al, 2019; Olejniczak-Staruch et al, 2021). A common way to identify the taxa of the microbiome between groups of interest is through 16S rRNA amplicon sequencing. Although many psoriasis microbiome studies utilized this method of sequencing, analyses varied in the following parameters: location of the specific variable region of the 16S amplicon (Abellan-Schneyder et al, 2021), differences in primer combinations, differences in bacterial extraction kits (Paniagua Voirol et al, 2021), differences by sequencing platform (Allali et al, 2017), and differences in bioinformatic pipelines and settings (Abellan-Schneyder et al, 2021; Allali et al, 2017). The variability in these parameters likely contributed to the contradictory findings published across reports, which showed different bacterial taxa that are significantly increased in psoriatic lesions (Gupta et al, 2022; Olejniczak-Staruch et al, 2021; Yan et al, 2017). Our aim was to perform a meta-analysis of all publicly available datasets utilizing a uniform bioinformatics pipeline and reference database to standardize our results and to generate robust associations of the skin microbiome with psoriasis by leveraging higher statistical power in an aggregated multivariable analysis.

[1]*The Lundquist Institute, Torrance, California, USA;* [2]*Division of Dermatology, Harbor-UCLA Medical Center, Torrance, California, USA; and* [3]*David Geffen School of Medicine, University of California Los Angeles, Los Angeles, California, USA*

Correspondence: Delphine J. Lee, Division of Dermatology, Harbor-UCLA Medical Center, 1000 W. Carson St, Box 458, Torrance, California 90502, USA. E-mail: delphine.lee@lundquist.org

Abbreviation: FC, fold change

Received 9 June 2023; revised 18 September 2023; accepted 24 October 2023; accepted manuscript published online 22 November 2023; corrected proof published online 9 January 2024

Cite this article as: JID Innovations 2024;4:100249

RESULTS

Sample description and distribution

Fourteen psoriatic microbiome studies were considered for analysis (Table 1). Publicly available data from 6 16S amplicon sequencing studies met the criteria for high-quality filtering, resulting in an aggregate of 977 skin swabs samples: 341 lesional, 295 nonlesional, and 341 from healthy sites. Project PRJNA281366 performed shotgun sequencing and was separate from our aggregate analyses because it was a different technique from 16S amplicon sequencing with different processing pipeline. Table 1 shows how the 16S

Table 1. Sequencing Projects on Psoriasis Microbiome

n of Patients	SRA Accession	First Author (y)	16S Region	Sequencing Platform	Extraction Kit	SwabBrand	Skin Sites
51	PRJNA46309	AV Alekseyenko 2013	V1V3	454 GS FLX	Mobio Powerlyzer	Epicentre Catch-All	Abdomen, elbow, knee, Scalp, face, hand
28	PRJEB25915	HW Chang 2018	V1V3	MiSeq	MasterPure Yeast	Epicentre Catch-All	Arm, leg, trunk, Axilla Buttock, Scalp
23	PRJEB14852	EA Langan 2019	V1V2	MiSeq	Powerlyzer UltraClean	Unknown	Scalp, umbilicus Elbow, knee
34	PRJNA483888	Z Stehlikova 2019	V1V2 V3V4	MiSeq	DNeasy PowerBiofilm	FLOQSwabs	Back, elbow
32	PRJEB42803	D Chen 2021	V3V4	NovaSeq	Mobio Powersoil	Epicentre Catch-All	Unknown
6	PRJEB29181	R Nijmegen —	V3V4	MiSeq	Unknown	Unknown	Trunk
28	PRJNA281366	A Tett 2017	Shotgun	HiSeq	Mobio Powersoil	VWR	Elbow, ear
134	PRJNA554499 (Errors)	N Fyhrquist 2019	V3V4	454 GS Titanium	QIAamp UCP Pathogen Mini	Unknown	Trunk
114	PRJNA427318 (No Data)	MA Loesche 2018	V1V3	MiSeq	Purelink Pro 96 Genomic Kit	Fisherbrand Synthetic Tip	Arm, axilla, buttock, leg, scalp, trunk
6	No Data	Z Gao 2008	V1V6	Unknown	DNeasy Tissue Kit	Unknown	Arm, elbow, leg, knee, trunk, extremities
10	No Data	A Fahlen 2012	V3V4	454 GS FLX	DNeasy Blood + Tissue	(Biopsy)	Trunk, arm, leg
1	No Data	L Drago 2016	V2V3	Ion Torrent	Genomic DNA Mini Kit	(Scrapes)	Unknown and Ear
27	No Data	C Quan 2019	V3V4	MiSeq	Plasmid Miniprep	Unknown	Extremities, buttocks, waist, head, face, trunk
39	No Data	M Assarsson 2020	V3V4	MiSeq	EZ1 Tissue Kit v2.0	ESwab	Elbow
39	No Data	C Jin-Young	V3	Ion Torrent S5 XL	QIAamp DNA Mini	Unknown	Scalp

The table presents the list of published manuscripts on psoriasis microbiome. Project PRJNA554499 was excluded owing to quality issues or errors with the upload. Loesche et al (2018) reported a project number (PRJNA427318), but the samples were not linked to any sequencing data as of December 12, 2023. Publicly available data from 6 amplicon sequencing and 1 shotgun sequencing were used in this study (the first 7 rows in the table).

sequencing projects vary in the rRNA variable region amplified, the sequencing platform (with different sequencing chemistry: colorspace vs basespace), brands of DNA extraction kits and swab material, and the body sites sampled (head, trunk, upper extremities, lower extremities, axilla, back, intergluteal fold). Such technical differences between projects translate into strong batch effects and biases between projects as illustrated by the beta-diversity ordination and Shannon alpha-diversity index in Figure 1. Samples also cluster together on the basis of the choice of 16S variable region and sequencing platform utilized.

The sample distribution and count across body sites, disease states, and projects are summarized in Table 2. Of note, the body sites sampled are not evenly balanced between projects and are unlabeled for PRJEB42803. Therefore, to preserve large sample size, our analyses do not explicitly adjust for body site parameters; partial adjustment is made by the overall batch correction between projects.

Microbial diversity by disease state

Alpha diversity by Shannon index was significantly higher in lesional and nonlesional samples from patients with psoriasis than from healthy controls ($P < .001$ and .003; signed fold change [FC] = 1.05 and 1.15) (Figure 2a); however, between lesional and nonlesional samples, the alpha diversity showed no difference, even by paired analysis ($P = .54$). Likewise, beta diversity by Bray–Curtis dissimilarity showed significant differences between lesional and healthy samples ($P < .001$, $R = 0.105$) and between nonlesional and healthy swabs ($P = .001$, $R = 0.078$) but not between lesional and nonlesional swabs ($P = .83$) (Figure 2b). Results remain consistent in sensitivity tests removing any one of the projects from the aggregate analysis.

Bacterial relative abundance by disease state

After reducing batch effect between projects and 16S variable region, we used MaAsLin2 to identify which bacteria are differentially abundant between psoriatic lesional, psoriatic nonlesional, and healthy samples. Boxplots of bacteria were statistically significant ($P < .05$) in 2 or more of the pairwise comparisons shown in Figure 3. Healthy skin swabs showed a higher relative abundance of *Cutibacterium acnes*, *Lawsonella* unclassified, and *Staphylococcus warneri* than samples from patients with psoriasis (Figure 3a) (healthy vs lesional $\log_2$FC = −0.55, −0.62, −0.53; healthy vs nonlesional $\log_2$FC = −0.27, −0.65, −0.36, respectively). On the other hand, samples from patients with psoriasis showed a higher relative abundance of *Acinetobacter* unclassified, *Acinetobacter johnsonii*, *Corynebacterium simulans*, *Corynebacterium* unclassified, *Neisseriaceae* unclassified, *S*

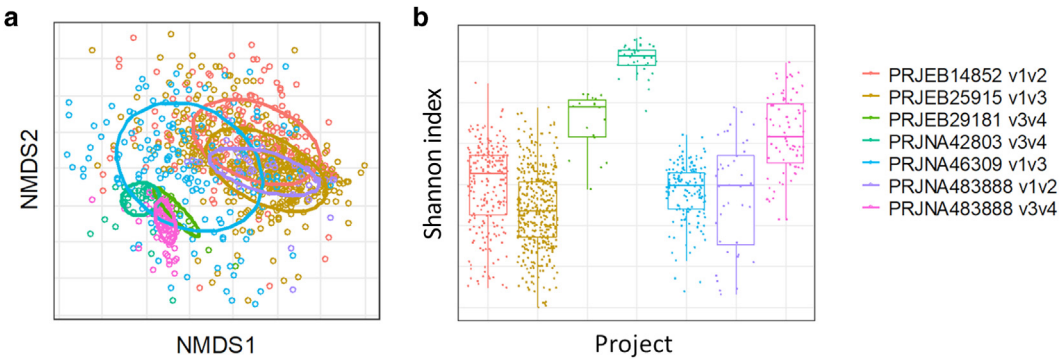

Figure 1. Beta and alpha diversity by project and 16S region. (**a**) Beta-diversity ordination and (**b**) Shannon alpha diversity across different projects and 16S variable region prior to batch effect corrections. NMDS, nonmetric multidimensional scaling.

Table 2. Sample Distribution Across Body Sites, Disease States, and Projects

Project ID		PRJEB14852	PRJEB25915	PRJEB29181	PRJEB42803	PRJNA46309	PRJNA483888	PRJNA483888
16S Variable Region		V1-V2	V1-V3	V3-V4	V3-V4	V1-V3	V1-V2	V3-V4
n-Patients	n-Psoriasis =	**23**	**28**	**6**	**26**	**51**	**7**	**25**
	n-Healthy =	**21**	**24**	**6**	**10**	**41**	**6**	**17**
Arm/Leg	Healthy	0	**52**	0	0	**1**	0	0
	Lesion	0	**48**	0	0	**15**	0	0
	Non-Lesion	0	**55**	0	0	**14**	0	0
Axilla	Healthy	0	**19**	0	0	0	0	0
	Lesion	0	**8**	0	0	0	0	0
	Non-Lesion	0	**24**	0	0	0	0	0
Back	Healthy	0	0	0	0	**2**	**9**	**11**
	Lesion	0	0	0	0	**8**	**15**	**20**
	Non-Lesion	0	0	0	0	**8**	**16**	**24**
Gluteal Crease	Healthy	0	**25**	0	0	0	0	0
	Lesion	0	**15**	0	0	0	0	0
	Non-Lesion	0	**27**	0	0	0	0	0
Face	Healthy	0	0	0	0	0	0	0
	Lesion	0	0	0	0	**1**	0	0
	Non-Lesion	0	0	0	0	**1**	0	0
Foot/Hand	Healthy	0	0	0	0	0	0	0
	Lesion	0	0	0	0	**2**	0	0
	Non-Lesion	0	0	0	0	**2**	0	0
Head	Healthy	**21**	**25**	0	0	**3**	0	0
	Lesion	**32**	**23**	0	0	**2**	0	0
	Non-Lesion	0	**25**	0	0	**2**	0	0
Knee/Elbow	Healthy	**38**	0	0	0	**44**	0	**8**
	Lesion	**26**	0	0	0	**20**	0	**6**
	Non-Lesion	**31**	0	0	0	**20**	0	**10**
Trunk	Healthy	**12**	**26**	**6**	0	**9**	0	0
	Lesion	**17**	**17**	**6**	0	**3**	0	0
	Non-Lesion	0	**27**	**6**	0	**3**	0	0
Umbilicus	Healthy	**20**	0	0	0	0	0	0
	Lesion	**31**	0	0	0	0	0	0
	Non-Lesion	0	0	0	0	0	0	0
Unknown	Healthy	0	0	0	**10**	0	0	0
	Lesion	0	0	0	**26**	0	0	0
	Non-Lesion	0	0	0	0	0	0	0

Number of swab samples with at least 2000 high-quality bacterial reads from across six amplicon sequencing projects (seven columns shown here, further subdividing project PRJNA483888 by its two 16S variable regions — V1V2 and V3V4). The first set of rows show the total number of psoriasis patients and healthy controls in each project (columns); The other rows are a list of body sites and how many of the samples were collected from a healthy, lesion, or non-lesion body site.

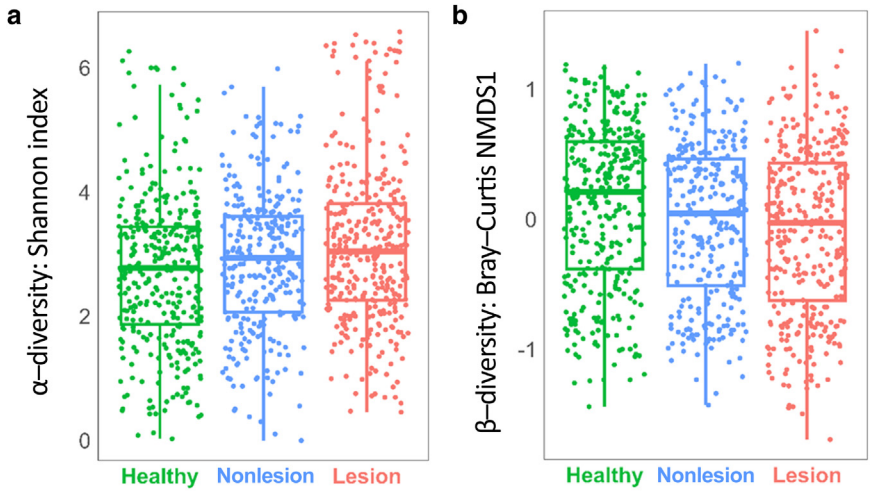

Figure 2. Microbiome diversity analysis between healthy, nonlesional, and lesional skin swab samples. Comparing (**a**) Shannon alpha diversity and (**b**) Bray–Curtis beta-diversity index between healthy (green), psoriasis nonlesional (blue), and psoriasis lesional (red). By generalized linear models, Shannon alpha diversity in lesional and nonlesional psoriasis samples was higher than in healthy skin ($P < .001$ and .003); however, there was no difference in alpha diversity between lesional and nonlesional skin ($P = .54$). Likewise, in the beta-diversity analysis, PERMANOVA test showed significant clustering between lesional and healthy samples ($P < .001$) and between nonlesional and healthy skin ($P = .001$) but no differences between lesional and nonlesional skin ($P = .83$). NMDS, nonmetric multidimensional scaling; PERMANOVA, Permutational multivariate ANOVA.

aureus, and *S caprae* (Figure 3b) (healthy vs lesional $\log_2$FC = 0.13, 0.24, 0.50, 0.15, 0.61, and 0.96, 0.87; healthy vs nonlesional $\log_2$FC = 0.74, 0.61, 0.45, 0.76, 0.64, 0.73, and 0.78, respectively). Lesional samples also had a higher relative abundance of *Acinetobacter* unclassified, *S aureus*, and *Corynebacterium* unclassified than nonlesional samples (nonlesional vs lesional $\log_2$FC = 0.30, 0.63, and 0.62, respectively).

A separate analysis by shotgun sequencing (PRJNA 281366), studying only psoriasis skin biopsies, compared lesional with nonlesional samples from patients with psoriasis. Nonlesional samples had a higher relative abundance of *C acnes*, *Kocuria indica*, and *A johnsonii* (adjusted $P < .05$); lesions had a higher relative abundance of *S aureus*, *S capitis*, and *C simulans* than nonlesions (adjusted $P < .05$) (Figure 4).

Microbiome by PASI scores

PASI score as a response variable was tested as a categorical variable (≤12 low PASI vs >12 high PASI) to preserve samples without the continuous PASI values. By 16S sequencing, the Shannon alpha diversity was higher with high PASI in lesional samples ($P = .041$), but alpha diversity was not significantly associated with PASI in nonlesional samples ($P = .59$). Next, we tested for bacteria associated with PASI scores for lesional and nonlesional samples in a combined analysis as well as separately. In the aggregated 16S analysis, which pooled lesional and nonlesional samples together, only *Porphyromonas* unclassified was statistically significant after false discovery correction, and it had higher relative abundance in patients with high PASI scores. *S warneri*, which was also associated with healthy samples, was associated with low PASI ($P < .05$) (Table 3). *C acnes* was associated with low PASI in just the lesional samples, and *S aureus* was associated with high PASI in the nonlesional samples ($P < .05$) (Figure 5). Similar results were obtained from the independent analysis of metagenomic sequencing data. *S aureus* and *C simulans* were associated with high PASI, and *C acnes* was associated with low PASI across both lesional and nonlesional samples (adjusted $P < .05$) (Table 4).

Bacterial pathway analysis

To investigate potential bacterial pathways that could be active at the site of skin sampling, we compared shotgun metagenomics sequencing data from lesional skin swab samples with those from nonlesional skin swab samples (adjusted $P < .05$) (Table 5). The top 3 pathways associated with lesional samples were superpathway of L-methionine biosynthesis (by sulfhydrylation), NAD salvage pathway II (PNC IV cycle), and L-methionine biosynthesis III. Associated with the nonlesional group was L-valine biosynthesis.

For 16S rRNA amplicon sequencing projects, PICRUSt2 was used to extrapolate microbiome pathways from bacterial count data on the basis of marker gene sequences. Although we found no differences in bacterial pathways when comparing lesional with nonlesional samples, we noted that healthy versus lesional samples revealed significantly different pathways after applying false discovery correction (Table 6). Two pathways were statistically significant across the following 3 analyses: (i) the aggregated 16S analysis comparing healthy with lesional skin swabs; (ii) the aggregated 16S analysis analyzing disease state as an ordinal variable, an ordered categorical variable progressing from healthy, nonlesional, and lesional (not shown); and (iii) the shotgun sequencing project mentioned earlier comparing nonlesional with lesional skin swabs. Across these 3 analyses, L-ornithine biosynthesis and L-histidine biosynthesis were lower in lesional samples (Figure 6).

Pathways were also compared between low PASI (≤12) and high PASI (>12) for both nonlesional and lesional samples together. The shotgun sequencing project showed that L-histidine degradation II and nitrate reduction V (assimilatory) were associated with low PASI (Table 7). However, in the aggregated analysis of 16S sequencing projects, none of the pathways were significantly different after correcting for

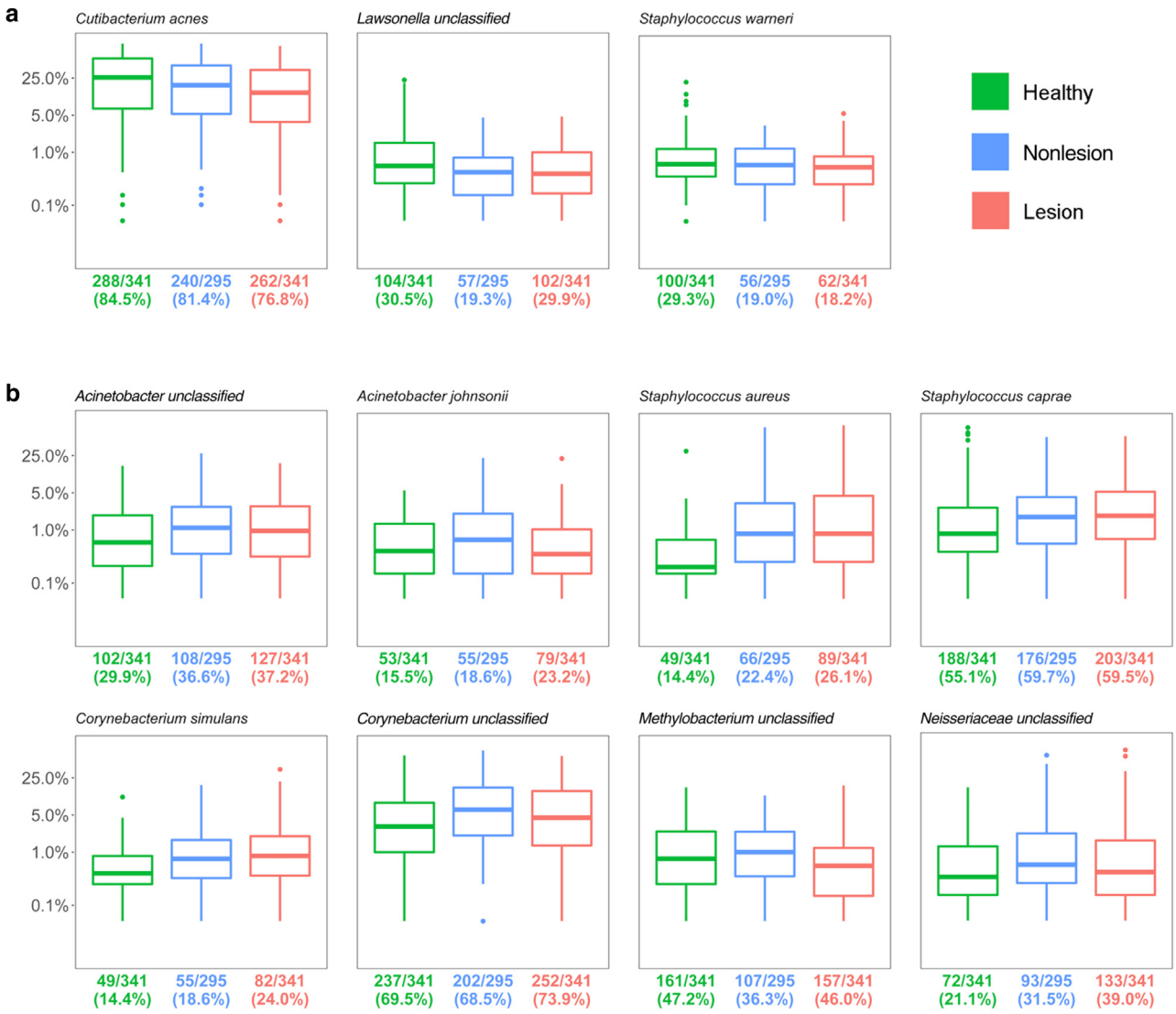

Figure 3. Comparing bacteria relative abundance between healthy, nonlesional, and lesion. Boxplots of bacteria were statistically significant ($P < .05$) in 2 or more of the pairwise comparisons (healthy, green; nonlesional, blue; lesional, red). X-axis at the bottom indicates the fraction and the percentage prevalence of the named bacteria. (**a**) Bacteria that had higher relative abundance in healthy skin swabs than in the skin of patients with psoriasis (both nonlesional and lesional swab samples). (**b**) Bacteria were significantly more abundant in patients with psoriasis than in healthy controls.

multiple hypothesis testing (Table 8). Without having applied false discovery correction, both approaches showed that high PASI was associated with sucrose degradation III (sucrose invertase).

DISCUSSION

In this study, our aggregate analysis reproduced some of the findings from the individual studies: the composition of the skin microbiome was significantly different between patients with psoriasis and normal healthy controls. We also confirmed the qualitative assessment by Gupta et al (2022) that psoriatic skin sites have greater heterogeneity (higher Shannon alpha diversity) than healthy skin. In addition, our analysis showed that lesional sites with higher PASI scores also had higher Shannon alpha diversity, further suggesting that greater bacterial heterogeneity (and possible loss of community stability) is associated with disease progression.

Of interest were the findings at the bacterial genus and species levels, which would otherwise be difficult to ascertain from individual papers owing to differences in sequence processing, reference databases, and methods for differential abundance analysis. Past studies have shown that *S aureus* colonizes psoriatic lesions in up to 60% of patients (Balci et al, 2009). In our aggregate analysis, *Staphylococcus* was differentially abundant by disease state, but with nuances: *S aureus* and *S caprae* were associated with skin swabs from patients with psoriasis, whereas *S warneri* was associated with healthy swabs, highlighting the importance of species-level taxonomic resolution. Notably, there was an incremental increase of *S aureus* and *C simulans* from healthy to nonlesional to lesional samples; conversely, there was an incremental decrease of *C acnes*, having the highest relative abundance in skin swabs from healthy individuals. Although past studies have also reported an increased relative abundance of *S aureus* in psoriasis skin versus in healthy skin (Chang et al,

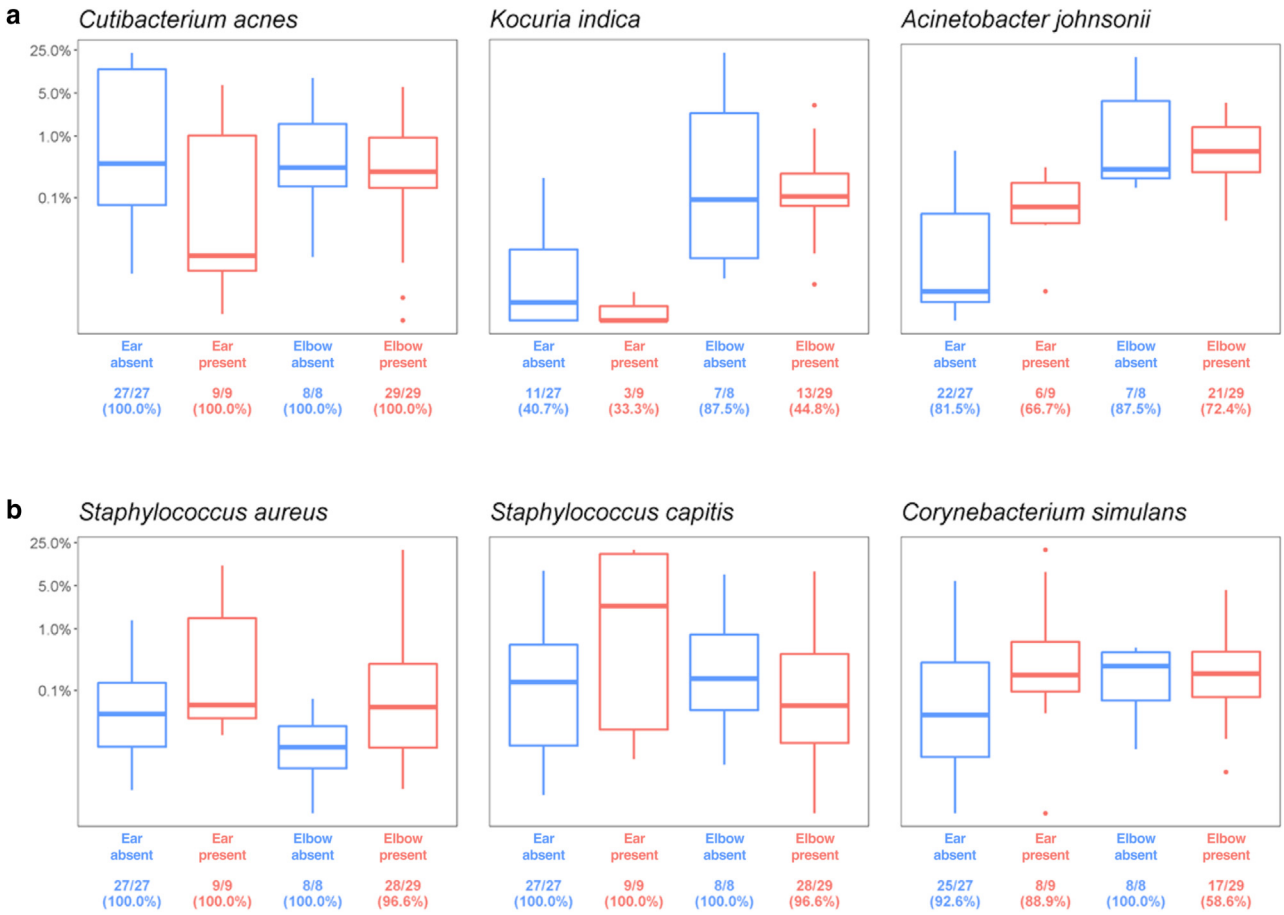

Figure 4. Bacteria differential abundance by shotgun sequencing. Reanalysis of whole-genome sequencing project PRJNA281366. Here, we combined the samples from ear and elbow to perform a multivariable analysis testing for bacteria significantly associated with psoriasis lesional (red) versus nonlesional (blue) samples. The multivariable analysis adjusted for the body site as well as the random effect from repeated samples from the same subject. The x-axis indicates the body site as well as the fraction and the percentage prevalence of the named bacteria in the group. (**a**) Bacteria with significantly higher relative abundance in nonlesional than in lesional skin (adjusted $P < .05$). (**b**) Bacteria with higher relative abundance in lesional than in nonlesional skin.

2018; Tett et al, 2017) and decreased relative abundance of *Cutibacterium* in the lesional skin (Fahlén et al, 2012; Gao et al, 2008), they did not demonstrate this incremental difference, with nonlesional skin being an intermediary.

Comparison by PASI scores in both lesional and nonlesional samples showed that *S aureus* and *C simulans* were associated with higher PASI scores, and *C acnes* was associated with lower PASI scores. These findings further support the notion that changes in the microbiota may be associated with psoriasis disease progression and may contribute to disease pathogenesis. Findings related to severe psoriasis were not driven by samples taken from moist body sites (such as inverted psoriasis) because the whole-genome sequencing project PRJNA281366 only collected samples from the ear and elbow.

The shift in microbiome composition may be explained by the decreasing levels of chemerin in the epidermis with psoriasis disease progression (Albanesi et al, 2009). Chemerin peptides are keratinocyte-derived factors with antimicrobial potential. Specifically, Chem157S can trigger chemotaxis of several types of immune cells (Yamaguchi et al, 2011) and inhibit the growth of bacteria such as *S aureus* and *C simulans* but not chemerin-resistant *C acnes* (Godlewska et al, 2020). With lower levels of chemerin in psoriatic lesions, *S aureus* and *C simulans* may have a growth advantage on the skin.

Several other mechanisms may explain the increased relative abundance of *C acnes* in healthy skin and the decreased relative abundance of *S aureus* and *Corynebacterium* in psoriasis. Propionic acids are a byproduct of *C acnes* metabolism and may help to modulate the pH levels, which would otherwise be elevated as observed in inflamed skin as well as aged and dry skin (Rozas et al, 2021). Their secretome contains RoxP (radical oxygenase of *Propionibacterium acnes*) protein, which has strong antioxidant properties and increases the viability of monocytes and keratinocytes exposed to oxidative stress (Andersson et al, 2019). *C acnes* also outcompete pathogens for nutrient acquisition by producing a thiopeptide antibiotic, cutimycin (Claesen et al, 2020). Finally, similarly to *S epidermidis*, *C acnes* has been shown to ferment glycerol to reduce methicillin-resistant *S aureus* (MRSA) growth (Shu et al, 2013).

The increase in *S aureus and C simulans* relative abundance in psoriatic skin may be related to their role in T helper 17 activation. *S aureus* proteins have been shown to promote T helper 17 differentiation in vitro, suggesting that colonization by *S aureus* can lead to increased T helper 17 activation and IL-17 secretion (Kolata et al, 2015). Teff cells

Table 3. Association Between PASI Scores and Bacteria by 16S rRNA Sequencing

Name	PASI	coef	stderr	pval	qval	N	N.not.zero
Porphyromonas unc.	> 12	1.74	0.46	< 0.001	0.025	267	105
Peptoniphilus unc.	> 12	1.36	0.45	0.004	0.090	267	153
Corynebacterium tuberculostearicum	> 12	1.23	0.61	0.047	0.388	267	198
Streptococcus unc.	> 12	1.17	0.57	0.042	0.380	267	188
Fenollaria unc.	> 12	0.91	0.42	0.034	0.336	267	71
Kocuria unc.	> 12	0.88	0.44	0.051	0.388	267	68
Saccharimonadales unc.	> 12	0.87	0.24	0.002	0.061	267	87
Stenotrophomonas unc.	> 12	0.87	0.35	0.016	0.236	267	87
P5D1-392 unc.	> 12	0.72	0.29	0.019	0.253	267	60
Pseudomonas synxantha	> 12	0.60	0.25	0.016	0.236	267	64
Fusobacterium unc.	> 12	0.52	0.24	0.034	0.336	267	64
Staphylococcus warneri	≤ 12	-0.78	0.37	0.044	0.381	267	71
Novosphingobium unc.	≤ 12	-1.10	0.35	0.002	0.061	267	80
Cutibacterium acnes	≤ 12	-1.22	0.69	0.079	0.488	267	212

This is the aggregated analysis of the 16S sequencing projects that pooled lesion and non-lesion psoriasis samples together and tested for differences in bacteria relative abundance between PASI low (≤ 12) versus PASI high (> 12). The pooled multivariable analysis adjusted for body site, disease state, and random effect from repeated sampling from the same patient. Only Poryphyromonas was significant after false discovery correction (Benjamini-Hochberg).

isolated from *S aureus*–colonized mice showed higher expression of IL-17A, IL-17F, and IL-22, cytokines that are implicated in psoriasis pathogenesis (Chang et al, 2018).

Corynebacterium is a major skin-resident bacteria and is generally considered a commensal bacteria under steady-state conditions, but little is known about the effects of *Corynebacterium* on host immunity. One study showed that *Corynebacterium*, through expression of mycolic acid in their cell envelops, may promote the production of IL-17A by γδ T17 cells, which is in part mediated by IL-23 (Ridaura et al, 2018).

Two biosynthesis pathways analyzed in this study may also be implicated in psoriasis pathogenesis. The L-ornithine biosynthesis pathway (GLUTORN-PWY) was lower in psoriatic lesions. L-ornithine is essential for the synthesis of

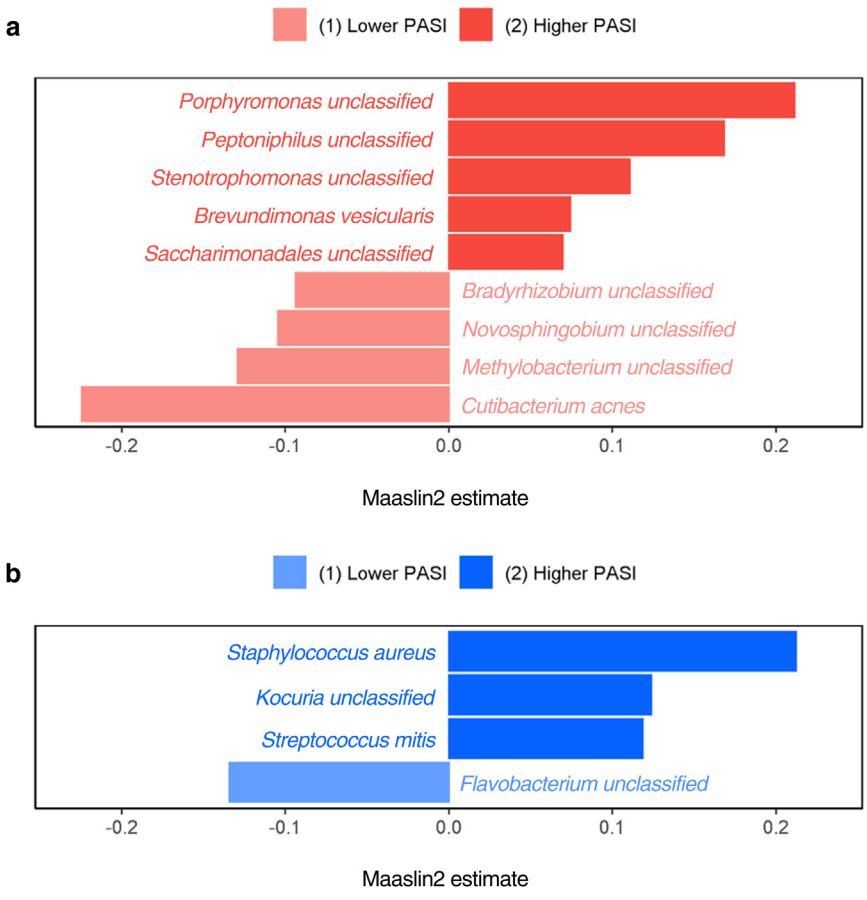

Figure 5. Bacteria associated with PASI score in psoriasis lesional swab samples by 16S analysis. Bacteria associated with PASI score in (**a**) lesional samples (red) and in (**b**) nonlesional samples (blue). Darker shade bars are for bacteria associated with higher PASI. Four of the 6 projects had PASI score data available (PRJEB14852, version 1v2; PRJEB29181, version 3v4; PRJEB42803, version 3v4; PRJNA46309, version 1v3; n lesional = 99, 6, 26, and 51; n nonlesional = 29, 6, 0, and 50).

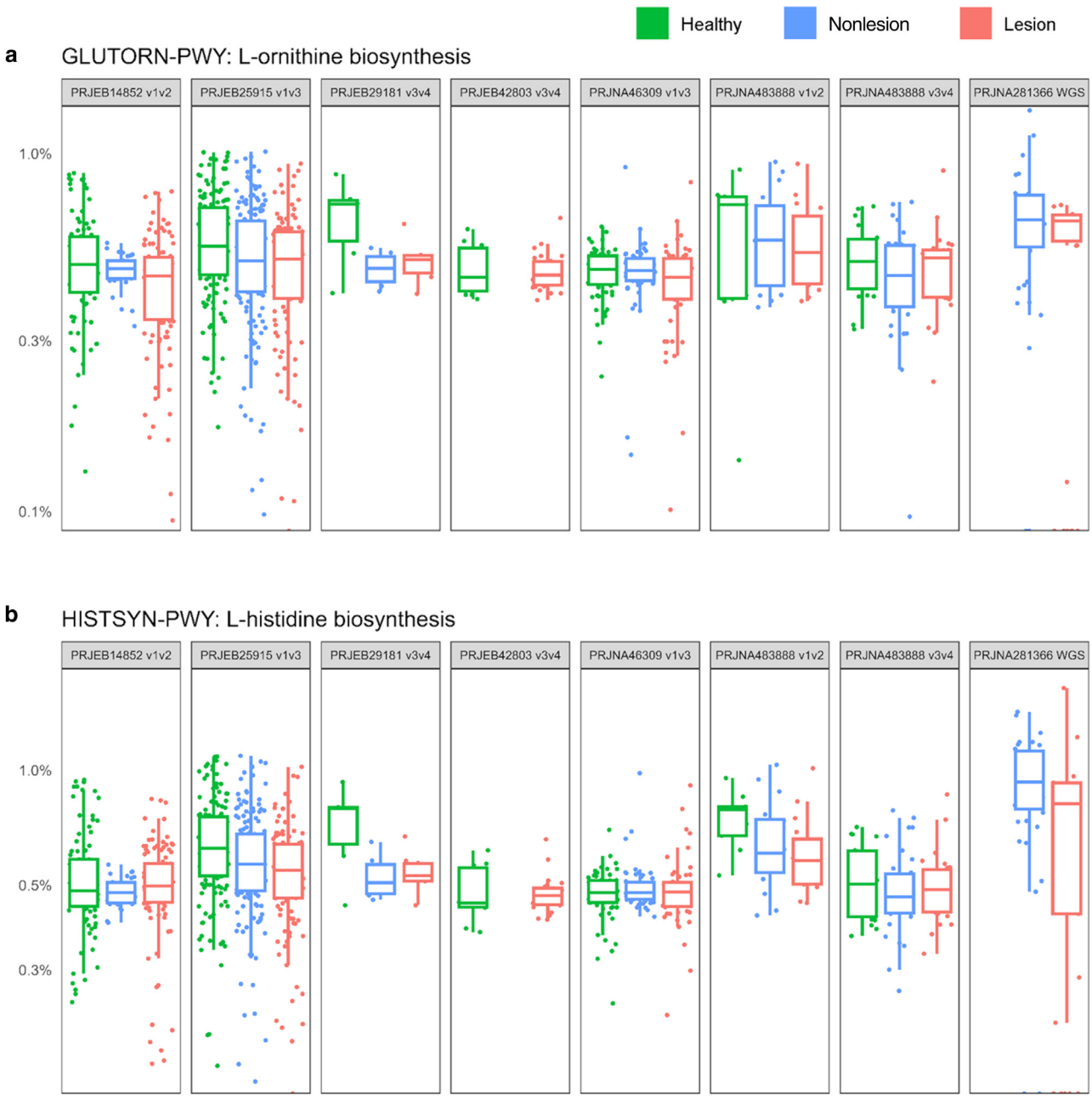

Figure 6. Pathways differentially abundant between disease states by both whole-genome sequencing and by 16S-PICRUSt prediction from marker genes. Boxplots of the 2 pathways that were significantly lower in lesional than in healthy skin across the 16S sequencing projects and significantly lower in lesional in the whole-genome sequencing project PRJNA281366 (adjusted $P < .05$). Y-axis shows the relative abundance of the pathway (**a**) L-ornithine biosynthesis and (**b**) L-histidine biosynthesis between healthy (green), nonlesional (blue), and lesional (red) across each psoriasis microbiome project.

polyamines that regulate cellular proliferation and differentiation. Metabolism of L-ornithine leads to a precursor of collagen synthesis, L-proline, which is important for wound healing (Wu and Morris, 1998). Additionally, N-iminoethyl-L-ornithine is an irreversible inhibitor of nitric oxide synthase in phagocytic cells (McCall et al, 1991); nitric oxide synthase is associated with M1 macrophages (Rath et al, 2014), which are associated with psoriatic lesions (PMID: 35837394).

The L-histidine biosynthesis pathway (HISTSYN-PWY) was also lower in the lesional samples. L-histidine's metabolites include *cis*-urocanic acid, which has been shown to be lower in psoriasis than in healthy controls (Yeh et al, 2023). Urocanic acid exists as a *trans*-isomer in the uppermost layer of the skin (stratum corneum) and has been proposed to act as a natural sunscreen, absorbing UVB before the damaging rays can penetrate lower epidermal zones (de fine Olivarius et al, 1996). Upon absorption of UV light, the naturally occurring *trans*-urocanic acid isomerizes to its *cis*-form (Kurimoto and Streilein, 1992). One of the proposed mechanisms underlying UVB therapy is the production of *cis*-urocanic acid by keratinocytes. *Cis*-urocanic acid may inhibit IL-23 expression and induce PD-L1 on Langerhans cells, leading to immunosuppression and improvement of psoriasis (Yeh et al, 2023). Lower levels of L-histidine in psoriasis may impact this proposed mechanism of immunosuppression.

One disadvantage of this study is the use of sequencing data, for which the results are compositional, meaning that the abundance features are all relative, and each bacterium's observed abundance is dependent on the observed abundance of all other measured bacteria. This contrasts with absolute abundance values, which factor in total bacterial load and would give a clearer interpretation of each feature and how they are different between biological states. However, approaches for absolute quantification are diverse and have their own set of challenges, including distinguishing between live and dead cells (Wang et al, 2021).

Other disadvantages of using 16S amplicon sequencing data are the PCR-related biases and errors associated with each of the variable regions (Kennedy et al, 2014). To address this, we performed covariate-controlled batch adjustments using MMUPHin and additionally adjusted for this effect in our multivariable analysis using MaAsLin2. Note that MMUPHin correction does not explicitly model PCR-related biases but rather simply adjusts for the overall variability between the different batches. A further disadvantage is that this short-read sequencing approach using a region on the 16S rRNA cannot achieve the taxonomic resolution afforded by sequencing the ~1500 base-pair segments (Johnson et al, 2019). Finally, pathway analysis using 16S sequencing data (PICRUSt2) is only predictive because it only infers the abundance of gene families on the basis of a database of the organism, its marker genes, and copy numbers. Shotgun sequencing provides greater gene coverage and more accurate functional profiling; only 1 shotgun sequencing project on psoriasis was publicly available.

There are a multitude of differential abundance methods, which, depending on the preprocessing method, would ultimately identify different numbers and sets of statistically significant bacteria. A study comparing the performance of such differential abundance methods found that the rarefied MaAsLin2 approach produced by far the most consistent results on the basis of a set of 5 datasets, which was particularly harder to interpret owing to their lower consistency (Nearing et al, 2022). Using the MaAsLin2 linear mixed model has the added advantage of not only being able to combine and adjust for the 6 datasets and possible covariates but also being able to adjust for repeated measures from the same subject. This is particularly important in our reanalysis of the shotgun sequencing project PRJNA281366. Rather than analyzing the 2 different body sites separately (eg, olecranon skin area [elbow] and retroauricular crease [ear]), our analysis combines all the samples in a mixed statistical model, adjusting for body site and random effects from repeated measures. Consequently, the results are more generalizable between psoriasis lesional and nonlesional sites but not specific to either the ear or the elbow (sebaceous or dry sites).

In summary, our study serves to pool the 6 available psoriasis microbiome datasets with 1 sequence-processing pipeline, 1 reference database, and 1 differential abundance method to evaluate which results are generalizable. The added statistical power of combining multiple datasets and a nuanced statistical model that accounted for batch effects and repeated measures contributed to a robust analysis. After aggregating datasets at the bacterial genus and species levels, our results confirmed that certain bacteria are associated with psoriasis skin versus healthy controls. However, we also showed an incremental increase in relative abundance of some bacteria with disease states and identified potential bacterial metabolic pathways in disease pathophysiology. These findings further support the notion that alterations in the microbiota may be associated with psoriasis pathogenesis and suggest potential targets for treatment.

MATERIALS AND METHODS

For the meta-analysis of psoriasis 16S sequencing projects, only baseline skin swab samples with sufficient high-quality reads were considered. To elaborate, a total of 1,063 skin samples were queried from 6 projects, and of the total, only swab samples were selected; this excluded 37 biopsies, 129 scrapes, and 10 unlabeled, all of which were from project PRJNA483888. Only baseline samples were selected, which excluded 74 samples from project PRJNA46309 collected at weeks 12 and 36 after adalimumab and or methotrexate treatment. Ultimately, 977 had at least 2000 high-quality bacterial reads for analysis: 341 healthy samples from 125 individuals and 341 lesional and 295 nonlesional swabs from 166 patients with psoriasis. Details of the sample distribution across body sites, disease states, and projects are summarized in Table 1.

Processing 16S amplicon sequencing reads

Fourteen psoriasis microbiome studies were considered. We included all publicly available datasets (Table 1) meeting the high-quality filtering criteria for DADA2 or mothur pipeline; standard methods for either pipeline do not allow ambiguous reads. Reads are truncated at the first instance of a quality score less than or equal to 28. Project PRJNA554499 was excluded because the reads upon truncation did not classify well against the SILVA reference database. Five of the published manuscripts did not have sequencing data associated with them. One other listed a project number (PRJNA427318) but with no data released (as of March 23, 2023).

DADA2, version 3.11, was used to process the sequencing data. Briefly, reads were filtered and trimmed using default parameters. DADA2 algorithm learns the error from each dataset to further denoise the sequencing reads. Chimeras are removed. Unique reads (amplicon sequencing variants) are assigned taxonomy against the SILVA, version 138.1, reference database. A total of 171 low-frequency singleton bacteria are removed. The remaining samples are rarefied to a sequencing depth of 2000 reads; 11 samples with an insufficient number of high-quality reads were omitted this way. Amplicon sequencing variant features were aggregated to their taxonomic classification by their sum.

PICRUSt2 (Phylogenetic Investigation of Communities by Reconstruction of Unobserved States) was used to predict bacterial pathway abundances using default settings. Samples with less than 2000 high-quality bacterial reads were excluded to be consistent with the bacterial composition analysis.

Processing whole-genome sequencing reads

There was 1 shotgun sequencing project with publicly available data for psoriasis skin swab samples (PRJNA281366) (Table 1); our analysis combines data from both the ear and the elbow in a multivariable analysis rather than analyzing them separately. HUMAnN3, version 3.0.1, pipeline was used to profile the microbial pathways abundance. Reads mapping to the reference human genome (hg37) were subtracted using kneaddata. Then, the forward and reversed reads were merged using fastp before finally mapping to ChocoPhlAn and UniRef90 database. Output tables were

renormalized into CPM (counts per million). Kraken2 was used for bacterial taxonomic classification using the prebuilt minikraken reference database (20200312). Bracken (Bayesian Reestimation of Abundance with KrakEN) computed the abundance of species in the DNA sequences.

Microbiome diversity analysis

Alpha diversity (effective number of species) was calculated using Shannon index before rarefaction to avoid loss of data; Shannon index is less dependent on library size because it takes into account both the total number of species and their abundances within a sample. Generalized linear model with binomial distributions was used to test the association between Shannon diversity (fixed effect). Beta-diversity analysis used Bray–Curtis dissimilarity index; ordination plots used nonmetric multidimensional scaling. Each point on the plot represents a sample, and the shorter distance between points show increasingly similar microbiome signature. Permutational multivariate ANOVA (adonis test) was performed on Bray–Curtis dissimilarities with stratification by the different projects and 16S variable regions to determine whether the samples from lesional, nonlesional, and healthy clustered by their beta-diversity partition distance

Statistical analysis

MMUPHIn (Meta-analysis Methods with a Uniform Pipeline for Heterogeneity in Microbiome Studies), version 1.2.0, was used to perform covariate-controlled batch and study effect adjustments for differential abundance testing. MMUPHIn reduced the batch effect between different projects while controlling for covariates such as the disease state of the samples (lesional, nonlesional, healthy). This method helps to keep the sample variation from disease states intact, thus preserving our study condition.

After reducing technical batch effects, multivariable analysis was performed using linear mixed-effect models with MaAsLin2 (Microbiome Multivariable Associations with Linear Models), version 1.2.0. MaAsLin2 sets the outcome variable as the per-feature taxa or PICRUSt2. The fixed effect being tested was the disease status (healthy, nonlesion, or lesional—subsetted for pairwise comparisons). Each model also contained random effects from the different projects and from repeated sampling from the same individual. Settings and options required at least 0.1% abundance from across 10% of the samples, and by default, MaAsLin2 also performs log transformation and total sum scaling normalization. False discovery correction was not applied to comparisons at the bacterial level; Benjamini–Hochberg correction was applied to comparisons of PICRUSt2 pathways between disease states.

PASI scores

PASI score was analyzed as a categorical variable (PASI $\leq$ 12 vs PASI $>$ 12) to preserve sample size; Project PRJEB42803, version 3v4, only had samples from lesions (lacking the nonlesional counterpart), and continuous PASI scores were not provided, only indicating that all their samples had PASI scores >12. In addition, a PASI threshold of 12 has been shown to be a justifiable cutoff to define a severe state of psoriasis (Schmitt and Wozel, 2005). In total, 4 of the 6 projects had PASI score data available (PRJEB14852, version 1v2; PRJEB29181, version 3v4; PRJEB42803, version 3v4; PRJNA46309, version 1v3; n lesional = 99, 6, 26, and 51; n nonlesional = 29, 6, 0, and 50). Differential abundance analyses by PASI scores were performed using MaAsLin2 linear mixed model with the detailed settings mentioned earlier. Lesional and nonlesional psoriasis samples were analyzed separately, and analyses were pooled together in a multivariable analysis. Each model contained random effects from the different projects and from repeated sampling from the same individual. The fixed effect being tested was PASI score; for the pooled analysis of both lesional and nonlesional samples, the model additionally included a fixed effect for the disease state.

ETHICS STATEMENT

Analysis was performed using publicly available sequencing data.

DATA AVAILABILITY STATEMENT

Analysis was performed using publicly available sequencing data.

ORCIDs

Alfred A. Chan: http://orcid.org/0009-0008-2866-6548
Patrick T. Tran: http://orcid.org/0000-0002-7417-085X
Delphine J. Lee: http://orcid.org/0000-0003-0063-5295

CONFLICT OF INTEREST

The authors state no conflict of interest.

ACKNOWLEDGMENTS

This work was supported in part by the Eastwood Charitable Trust. The authors received no financial support for the research, authorship, and/or publication of this article. The team would like to thank Jennifer Chung Chen for her edits and insightful questions for discussion.

AUTHOR CONTRIBUTIONS

Conceptualization, Data Curation, Formal Analysis, Methodology, Visualization: AAC, DJL; Software: AAC; Supervision: DJL; Writing - Original Draft Preparation, Writing - Review and Editing: AAC, PTT, DJL.

SUPPLEMENTARY MATERIALS

Supplementary material is linked to the online version of the paper at www.jidonline.org, and at https://doi.org/10.1016/j.xjidi.2023.100249.

REFERENCES

Abellan-Schneyder I, Matchado MS, Reitmeier S, Sommer A, Sewald Z, Baumbach J, et al. Primer, pipelines, parameters: issues in 16S rRNA gene sequencing. mSphere 2021;6:e01202–20.

Albanesi C, Scarponi C, Pallotta S, Daniele R, Bosisio D, Madonna S, et al. Chemerin expression marks early psoriatic skin lesions and correlates with plasmacytoid dendritic cell recruitment. J Exp Med 2009;206:249–58.

Allali I, Arnold JW, Roach J, Cadenas MB, Butz N, Hassan HM, et al. A comparison of sequencing platforms and bioinformatics pipelines for compositional analysis of the gut microbiome. BMC Microbiol 2017;17:194.

Andersson T, Ertürk Bergdahl G, Saleh K, Magnúsdóttir H, Stødkilde K, Andersen CBF, et al. Common skin bacteria protect their host from oxidative stress through secreted antioxidant RoxP. Sci Rep 2019;9:3596.

Balci DD, Duran N, Ozer B, Gunesacar R, Onlen Y, Yenin JZ. High prevalence of *Staphylococcus aureus* cultivation and superantigen production in patients with psoriasis. Eur J Dermatol 2009;19:238–42.

Carmona-Cruz S, Orozco-Covarrubias L, Sáez-de-Ocariz M. The human skin microbiome in selected cutaneous diseases. Front Cell Infect Microbiol 2022;12:834135.

Chang HW, Yan D, Singh R, Liu J, Lu X, Ucmak D, et al. Alteration of the cutaneous microbiome in psoriasis and potential role in Th17 polarization. Microbiome 2018;6:154.

Chen L, Li J, Zhu W, Kuang Y, Liu T, Zhang W, et al. Skin and gut microbiome in psoriasis: gaining insight into the pathophysiology of it and finding novel therapeutic strategies. Front Microbiol 2020;11:589726.

Claesen J, Spagnolo JB, Ramos SF, Kurita KL, Byrd AL, Aksenov AA, et al. A *Cutibacterium acnes* antibiotic modulates human skin microbiota composition in hair follicles. Sci Transl Med 2020;12:eaay5445.

de fine Olivarius F, Wulf HC, Crosby J, Norval M. The sunscreening effect of urocanic acid. Photodermatol Photoimmunol Photomed 1996;12:95–9.

Fahlén A, Engstrand L, Baker BS, Powles A, Fry L. Comparison of bacterial microbiota in skin biopsies from normal and psoriatic skin. Arch Dermatol Res 2012;304:15–22.

Gao Z, Tseng CH, Strober BE, Pei Z, Blaser MJ. Substantial alterations of the cutaneous bacterial biota in psoriatic lesions. PLoS One 2008;3:e2719.

Godlewska U, Bilska B, Majewski P, Pyza E, Zabel BA, Cichy J. Bacteria modify their sensitivity to chemerin-derived peptides by hindering peptide association with the cell surface and peptide oxidation. Front Microbiol 2020;11:1819.

Gupta M, Weinberg JM, Yamauchi PS, Patil A, Grabbe S, Goldust M. Psoriasis: embarking a dynamic shift in the skin microbiota. J Cosmet Dermatol 2022;21:1402–6.

Johnson JS, Spakowicz DJ, Hong BY, Petersen LM, Demkowicz P, Chen L, et al. Evaluation of 16S rRNA gene sequencing for species and strain-level microbiome analysis. Nat Commun 2019;10:5029.

Kennedy K, Hall MW, Lynch MD, Moreno-Hagelsieb G, Neufeld JD. Evaluating bias of Illumina-based bacterial 16S rRNA gene profiles. Appl Environ Microbiol 2014;80:5717–22.

Kolata JB, Kühbandner I, Link C, Normann N, Vu CH, Steil L, et al. The fall of a dogma? Unexpected high T-cell memory response to *Staphylococcus aureus* in humans. J Infect Dis 2015;212:830–8.

Kurimoto I, Streilein JW. Deleterious effects of cis-urocanic acid and UVB radiation on Langerhans cells and on induction of contact hypersensitivity are mediated by tumor necrosis factor-alpha. J Invest Dermatol 1992;99:69S–70S.

Lewis DJ, Chan WH, Hinojosa T, Hsu S, Feldman SR. Mechanisms of microbial pathogenesis and the role of the skin microbiome in psoriasis: a review. Clin Dermatol 2019;37:160–6.

Loesche MA, Farahi K, Capone K, Fakharzadeh S, Blauvelt A, Duffin KC, et al. Longitudinal study of the psoriasis-associated skin microbiome during therapy with Ustekinumab in a randomized phase 3b clinical trial. J Invest Dermatol 2018;138:1973–81.

Mazur M, Tomczak H, Lodyga M, Czajkowski R, Żaba R, Adamski Z. The microbiome of the human skin and its variability in psoriasis and atopic dermatitis. Postepy Dermatol Alergol 2021;38:205–9.

McCall TB, Feelisch M, Palmer RM, Moncada S. Identification of N-iminoethyl-L-ornithine as an irreversible inhibitor of nitric oxide synthase in phagocytic cells. Br J Pharmacol 1991;102:234–8.

Nearing JT, Douglas GM, Hayes MG, MacDonald J, Desai DK, Allward N, et al. Microbiome differential abundance methods produce different results across 38 datasets [published correction appears in Nat Commun 2022;13:777. Nat Commun 2022;13:342.

Olejniczak-Staruch I, Ciążyńska M, Sobolewska-Sztychny D, Narbutt J, Skibińska M, Lesiak A. Alterations of the skin and gut microbiome in psoriasis and psoriatic arthritis. Int J Mol Sci 2021;22:3998.

Paniagua Voirol LR, Valsamakis G, Yu M, Johnston PR, Hilker M. How the 'kitome' influences the characterization of bacterial communities in lepidopteran samples with low bacterial biomass. J Appl Microbiol 2021;130:1780–93.

Rath M, Müller I, Kropf P, Closs EI, Munder M. Metabolism via arginase or nitric oxide synthase: two competing arginine pathways in macrophages. Front Immunol 2014;5:532.

Ridaura VK, Bouladoux N, Claesen J, Chen YE, Byrd AL, Constantinides MG, et al. Contextual control of skin immunity and inflammation by *Corynebacterium*. J Exp Med 2018;215:785–99.

Rozas M, Hart de Ruijter A, Fabrega MJ, Zorgani A, Guell M, Paetzold B, et al. From dysbiosis to healthy skin: major contributions of *Cutibacterium acnes* to skin homeostasis. Microorganisms 2021;9:628.

Schmitt J, Wozel G. The psoriasis area and severity index is the adequate criterion to define severity in chronic plaque-type psoriasis. Dermatol (Basel Switzerland) 2005;210:194–9.

Shu M, Wang Y, Yu J, Kuo S, Coda A, Jiang Y, et al. Fermentation of *Propionibacterium acnes*, a commensal bacterium in the human skin microbiome, as skin probiotics against methicillin-resistant *Staphylococcus aureus*. PLoS One 2013;8:e55380.

Tett A, Pasolli E, Farina S, Truong DT, Asnicar F, Zolfo M, et al. Unexplored diversity and strain-level structure of the skin microbiome associated with psoriasis. NPJ Biofilms Microbiomes 2017;3:14.

Wang X, Howe S, Deng F, Zhao J. Current applications of absolute bacterial quantification in microbiome studies and decision-making regarding different biological questions. Microorganisms 2021;9:1797.

Wu G, Morris SM Jr. Arginine metabolism: nitric oxide and beyond. Biochem J 1998;336:1–17.

Yamaguchi Y, Du XY, Zhao L, Morser J, Leung LL. Proteolytic cleavage of chemerin protein is necessary for activation to the active form, Chem157S, which functions as a signaling molecule in glioblastoma. J Biol Chem 2011;286:39510–9.

Yan D, Issa N, Afifi L, Jeon C, Chang HW, Liao W. The role of the skin and gut microbiome in psoriatic disease. Curr Dermatol Rep 2017;6:94–103.

Yeh CY, Su SH, Tan YF, Tsai TF, Liang PH, Kelel M, et al. PD-L1 enhanced by cis-urocanic acid on Langerhans cells inhibits Vγ4(+) γδT17 cells in psoriatic skin inflammation. J Invest Dermatol 2023;143:1449–60.